JOURNAL OF GENERAL VIROLOGY

RESEARCH ARTICLE

Oliveira Leastro *et al.*, *Journal of General Virology* 2022;103:001805

DOI 10.1099/jgv.0.001805

MICROBIOLOGY SOCIETY

Orchid fleck dichorhavirus movement protein shows RNA silencing suppressor activity

Mikhail Oliveira Leastro*, Vicente Pallás and Jesús Ángel Sánchez-Navarro*

Abstract

To counteract RNA interference-mediated antiviral defence, virus genomes evolved to express proteins that inhibit this plant defence mechanism. Using six independent biological approaches, we show that orchid fleck dichorhavirus citrus strain (OFV-citrus) movement protein (MP) may act as a viral suppressor of RNA silencing (VSR). By using the alfalfa mosaic virus (AMV) RNA 3 expression vector, it was observed that the MP triggered necrosis response in transgenic tobacco leaves and increased the viral RNA (vRNA) accumulation. The use of the potato virus X (PVX) expression system revealed that the *cis* expression of MP increased both the severity of the PVX infection and the accumulation of PVX RNAs, further supporting that MP could act as an RNA silencing suppressor (RSS). From the analysis of the RSS-defective turnip crinkle virus (TCV), we do not find local RSS activity for MP, suggesting a link between MP suppressor activity and the prevention of systemic silencing. In the analysis of local suppressive activity using the GFP-based agroinfiltration assay in *Nicotiana benthamiana* (16 c line), we do not identify local RSS activity for the five OFV RNA1-encoded proteins. However, when evaluating the small interfering RNA (siRNA) accumulation, we find that the expression of MP significantly reduces the accumulation of GFP-derived siRNA. Finally, we examine whether the MP can prevent systemic silencing in 16c plants. Our findings show that MP inhibits the long-distance spread of RNA silencing, but does not affect the short-distance spread. Together, our findings indicate that MP is part of OFV's counter-defence mechanism, acting mainly in the prevention of systemic long-distance silencing. This work presents the first report of a VSR for a member of the genus *Dichorhavirus*.

INTRODUCTION

RNA silencing is a nucleotide sequence-specific gene regulation mechanism that acts as a primary defence pathway in many eukaryotic cells. It defends a large number of organisms against virus infection [1, 2]. The RNA silencing defence mechanism is triggered by the presence of double-stranded RNA that is processed by an RNase III Dicer-like nuclease to generate small RNA (siRNA) duplexes of 21 to 24 nucleotide (nt) in size [3–5]. They are incorporated into a nuclease named Argonaute (AGO), which is able to select an RNA strand of Dicer-generated short RNA duplex (guide strand) by a thermodynamic mechanism to guide the AGO complex to cleave specific nucleic acids or to modify chromatin structure [4, 6–8]. To counteract this antiviral defence mechanism, viruses have evolved to encode proteins called viral suppressors of RNA silencing (VSRs) [9–12]. These proteins

Received 18 August 2022; Accepted 13 October 2022; Published 18 November 2022

Author affiliations: [1]Instituto de Biología Molecular y Celular de Plantas, Universidad Politécnica de Valencia-Consejo Superior de Investigaciones Científicas (CSIC), Valencia 46022, Spain.

***Correspondence:** Mikhail Oliveira Leastro, m.leastro@gmail.com; Jesús Ángel Sánchez-Navarro, jesanche@ibmcp.upv.es

Keywords: dichorhavirus; OFV; movement protein; RNA silencing; viral suppressors of RNA silencing.

Abbreviations: ADV, alfalfa dwarf cytorhabdovirus; AGO, Argonaute; AMV, alfalfa mosaic virus; BBWV-1, broad bean wilt virus 1; bp, base pairs; BTVs, *Brevipalpus*-transmitted viruses; BYSMV, barley yellow striate mosaic cytorhabdovirus; CaMV, cauliflower mosaic virus; CarMV, carnation mottle virus; CiLV-C, citrus leprosis virus C; CL, citrus leprosis; CMV, cucumber mosaic virus; CP, coat protein; g, genomic; G, glycoprotein; GFP, green fluorescent protein; HA, human influenza haemagglutinin epitope; HCPro, helper component proteinase; L, RNA-dependent- RNA polymerase; LB, Luria–Bertani; LNYV, lettuce necrotic yellows cytorhabdovirus; M, matrix protein; MMDaV, mulberry mosaic dwarf-associated geminivirus; MP, movement protein; N, nucleocapsid; OFV, orchid fleck virus; P, phosphoprotein; P12, transgenic tabacum plant; PCD, programmed cell death; p.i., post-inoculation; PoPit, potato proteinase inhibitor; PTGS, post-transcriptional gene silencing; PVX, potato virus X; RDR6, RNA-dependent RNA polymerase 6; RdRp, polymerase; ROS, reactive oxygen species; RSS, RNA silencing suppressor; RYSV, rice yellow stunt alphanucleorhabdovirus; 35S, promoter from CaMV; SD, standard deviations; sg, subgenomic; SGS3, suppressor of gene silencing 3; siRNA, small interfering RNA; TBSV, tomato bushy stunt virus; TCV, turnip crinkle virus; TEV, tobacco etch virus; TGB1-3, triple gene block; TLS, tRNA-like structure; ULs, upper leaves; VSR, viral suppressor of RNA silencing; WT, Wild Type.

Four supplementary figures are available with the online version of this article.

exhibit no obvious sequence similarities and may act in different steps of RNA silencing by interacting with key components of the local and systemic silencing machinery [11, 13–16].

Using different biological approaches, it has been possible to identify a larger number of viral proteins that act as silencing suppressors [9, 17–20]. The best-known technology to test the ability of the protein to suppress local RNA silencing is the 'patch' technique [21]. It consists of the use of an inductor for gene silencing (the most used is green fluorescent protein, GFP) co-overexpressed in plants with a putative RSS by agrobacterial delivery. This technology has also been used extensively to assess the influence of the putative VSRs on the accumulation of siRNAs and the short- and long-distance spread of the silencing signal [15, 18, 19, 22–25]. Plant virus genomes have been engineered for the development of viral infectious clones used for RSS screening. By using alfalfa mosaic virus (AMV) as an expression vector, a correlation between necrotic lesion, increase of viral RNA (vRNA) accumulation and RSS activity was observed [18]. For the potato virus X (PVX) system, the RSS activity is associated with the enhancement of PVX pathogenicity [9]. In the case of the turnip crinkle virus (TCV) system, the expression of an RSS is associated with the local movement complementation of a defective TCV mutant [17].

Citrus leprosis (CL) is an important disease for the citrus industry in South and Central America that is caused by *Brevipalpus*-transmitted viruses (BTVs). According to the cytopathological patterns they provoke in infected tissues, BTVs can be grouped into two distinct groups. The cytoplasmic type (BTV-C) is composed by viruses belonging to the genus *Cilevirus*, family *Kitaviridae*, able to replicate in the host cell cytoplasm [26]. Members of the nuclear type (BTV-N) replicate into the cell nuclei and belong to the genus *Dichorhavirus*, family *Rhabdoviridae* [27]. Orchid fleck virus (OFV orchid strain) is the type member of the genus *Dichorhavirus* and shows a worldwide distribution [27]. By contrast, the citrus strain of OFV (OFV-citrus), associated with the infection of citrus plants causing typical CL symptoms, has been found in South Africa and Central America [28–30]. Dichorhaviruses show negative-stranded RNA bisegmented genomes, which code for the nucleocapsid (N), phosphoprotein (P), movement protein (MP), matrix protein (M), glycoprotein (G) and RNA-dependent-RNA polymerase (L). The N, P, MP, M, and G proteins are encoded by the RNA1, while the RNA 2 codes for the L protein (Fig. S1, available in the online version of this article) [27, 31]. OFV nucleocapsid proteins (N and P) form an intranuclear viroplasm-like structure mediated by P nuclear localization signal [32]. The MP is a membrane-associated protein, while the N is not associated to cell membranes. The MP can interact with the N–P core complex, redirecting a portion of the N from the nucleus to the plasmodesmata at the cell periphery [33]. As regards its intracellular distribution, the MP shows a nuclear localization that is also distributed at the cell periphery, co-localizing with plasmodesma structures [33].

Dichorhaviruses share some similarities, including composition of structural proteins, gene order, moderate to high sequence similarity, and nuclear localization, with non-segmented plant rhabdoviruses, especially with the alpha, beta and gamma nucleorhabdoviruses [27, 31, 34]. For rhabdoviruses, conserved structural protein (P) and accessory gene-encoded proteins (P6 and P3) have been identified as acting as VSRs by interacting with components of the local and/or systemic RNA silencing machinery [35–39]. Although current studies have advanced the understanding of the molecular processes associated with the suppressive activity of proteins encoded by rhabdoviruses, this same progress has not been reported for dichorhaviruses, which are evolutionarily close to this group.

In the present work, using six independent biological methods to screen the local or systemic RSS activity of viral proteins, we found that the OFV-citrus MP may act as an RNA silencing suppressor, possibly inhibiting the long-distance spread of RNA silencing.

METHODS

Plant materials

Transgenic *Nicotiana benthamiana* 16 c plants that constitutively express the green fluorescent protein (GFP) [40] were used for analyses of local and systemic RNA silencing. For the analysis of local silencing, the plants were kept in fitotron plant growth chambers under growing conditions that included a two-step cycle of 23 °C day/18 °C night and 16 h light/8 h dark. For analysis of systemic silencing, the conditions were changed to 20 °C day/18 °C night and 14 h light/10 h dark. At higher light intensities and temperatures, the spread of systemic silencing signal is impaired. By contrast, lower light intensities with a constant temperature generate a strong systemic movement of the silencing signal [41].

Transgenic *Nicotiana tabacum* plants that express the polymerase proteins P1 and P2 (P12 plants) of alfalfa mosaic virus (AMV) [42] were used to identify potential RNA silencing suppressor (RSS) activity of the assayed proteins by using the AMV system. The P12 plants only work with the AMV RNA 3 or its derivatives, simplifying the analysis [43]. P12 plants grew under a two-step cycle of 23 °C day/18 °C night and 16 h light/8 h dark.

N. benthamiana wild-type (WT) plants grew in the same conditions described above and were employed for the analyses using the viral systems of the potato virus X (PVX) [44] and turnip crinkle virus (TCV) [17].

Generation of constructs and biological assays

Constructs for alfalfa mosaic system and AMV assay

A derivative infectious AMV RNA 3 construct that carries the *GFP* gene (pGFP/MP/CP) [45] allows the exchange of the *GFP* gene to test the potential RSS proteins. *Nco*I and *Nhe*I cutting sites ensure *GFP* removal. The nucleocapsid (*N*), phosphoprotein (*P*), matrix protein (*M*), movement protein (*MP*) and glycoprotein (*G*) genes of the orchid fleck virus citrus strain (OFV-citrus) (isolate M2345, GenBank accession no. KF209275.2) were obtained from RNA extracted from symptomatic citrus leaves. The cDNA was generated by RT-PCR following the manufacturer's specifications (Thermo Fisher Scientific, Waltham, MA, USA) with specific primers for each OFV-citrus gene. PCR amplification was performed with primers carrying the sites *Nco*I and *Xba*I (*N*), *Pci*I and *Nhe*I (*P* and *M*), and *BspH*I and *Nhe*I (*MP* and *G*). The derivative PCR products, previously digested, were cloned into the pGFP/MP/CP plasmid to generate p*N*/MP/CP, p*P*/MP/CP, p*MP*/MP/CP, p*M*/MP/CP and p*G*/MP/CP constructs. p*HCPro*/MP/CP and pHA:*HCPro*/MP/CP constructs used as control were obtained from Ref. [18]. The helper component proteinase HCPro is a VSR from the tobacco etch virus (TEV) (GenBank accession no. DQ986288). The introduction of the human influenza haemagglutinin epitope (HA) at the C-terminus of the heterologous inserted proteins for protein detection was performed as previously described [18].

For the AMV assay, the cassettes from AMV RNA 3 (pGFP/MP/CP plasmid) harbouring the genes from encoded proteins *HCPro* (control), *N*, *P*, *MP*, *M* and *G* were amplified with specific pair primers and the generated amplicons were used as templates for *in vitro* transcription with T7 RNA polymerase (Takara Bio, Inc., Shiga, Japan). We first balanced the concentration of AMV RNA 3 transcripts carrying the heterologous indicated genes. The quantification was performed with agarose gel electrophoresis using an RNA ladder (RiboRuler High Range RNA Ladder, Thermo Scientific, USA) and several dilutions of the transcribed RNAs [46]. The transcripts generated (~3 µg) were used for inoculation of transgenic P12 plants at 2–4 weeks old (two leaves per plant and three plants per construct in three independent experiments), as described previously [47]. The presence of necrotic lesions on the inoculated leaves was monitored during 7 days post-inoculation (p.i.).

P12 protoplast transfection was performed as described previously [48]. Briefly, protoplasts were extracted from P12 leaves (3-week-old plants) and 2.5×10^5 protoplasts were transfected by the polyethylene glycol method [48] with 15 µl (~ 3 µg) of the transcription mixture [19].

Constructs for potato virus X system and PVX assay

The *MP* gene carrying *Asc*I and *Not*I restriction sites was introduced into the pGR106 plasmid [44], downstream of the duplicated PVX CP promoter [49]. This plasmid was a gift from Dr Zhenghe Li (Zhejiang University, Faculty of Agriculture, Hangzhou, PR China). pGR107 carrying the HCPro gene was obtained from Ref. [19].

For the PVX assay, pGR empty (pGR106-empty) and carrying the *HCPro* (pGR107-HCPro) and *MP* (pGR106-MP) genes were used for the transformation of *Agrobacterium tumefaciens* strain C58C1 harbouring the helper plasmid pSoup [50]. Individual agrobacterium cultures grew at 28 °C in Luria–Bertani (LB) medium containing rifampicin (100 mg ml^{-1}) and kanamycin (50 mg ml^{-1}) antibiotics for plasmid and agrobacterium selection. At the four-leaf growth stage, *N. benthamiana* leaves (three plants per construct in three independent experiments) were agroinfiltrated (OD_{600}=0.5) with the PVX derivatives: PVX-empty (negative control), PVX-HCPro (positive control) and PVX-MP. Next, at 3 days p.i., agroinfiltrated leaves were crushed in phosphate buffer (30 mM, pH 8.0) and the leaf extract was used as virus particle inoculum for mechanical inoculation of new *N. benthamiana* using Carborundum (VWR prolabo, France) as an abrasive. The PVX pathogenicity (symptom development) from plants agroinfiltrated and mechanically inoculated was monitored up to 30 days post-infiltration or -inoculation.

Constructs for turnip crinkle virus system and TCV assays

The movement-defective TCV-sGFP clone, used for the TCV-sGFP complementation assay, shows a deletion of the coat protein (CP) gene, containing an sGFP in the place of the CP. TCV CP does not have an inherent movement function but acts as a VSR [17]. Potential RSS activity is identified by the capacity of the protein tested to rescue the TCV movement. The pZP-TCV-sGFP binary construct, used for the co-infiltration assay, also presents this exchange of the CP by sGFP. In this case, the presence of RSS activity is associated with an increase of the GFP signal [17]. The construction of both clones was described previously [18].

For the TCV complementation assay, the movement-deficient phenotype of a TCV CP deletion mutant that expresses the sGFP is rescued *in trans* by the transient expression of an RSS. At the six-leaf growth stage, *N. benthamiana* leaves (two leaves per plant and three plants per construct) were agroinfiltrated (OD_{600}=1) with cultures (strain C58C1) transformed with pMOG empty or carrying HCPro (controls) or the MP gene from OFV-citrus. One day post-agroinfiltration, the abaxial surfaces of the leaves were mechanically inoculated with RNA transcripts (~3 µg) obtained from the pTCV-sGFP plasmid, from its linearization using *Xba*I and subsequent transcription with T7 RNA polymerase (Takara Bio, Inc., Shiga, Japan) [18]. At 3 days p.i., the possible rescue of the TCV movement was evaluated by GFP excitation from UV light exposure using a Leica MZ16F (Wetzlar, Germany) fluorescence stereomicroscope.

For the co-infiltration assay, the presence of RSS activity is evaluated by co-infiltration of the tested protein cloned in a binary vector with a pZP-TCV-sGFP binary construct. At the six-leaf growth stage, *N. benthamiana* leaves (three leaves per plant and three plants per agrobacterium culture combination) were co-infiltrated as a mix of *A. tumefaciens* cultures individually transformed with pZP-TCV-sGFP binary construct and the pMOG constructs mentioned below. For agrobacterium culture carrying the pZP-TCV-sGFP plasmid the OD_{600} was adjusted to 0.0025 [17], while for cultures containing the pMOG it was OD_{600}=1.0. The GFP signal was monitored at 5 days p.i. with a Leica MZ16F (Wetzlar, Germany) fluorescence stereomicroscope. Each TCV assay was repeated three times.

Constructs for ectopic expression and *N. benthamiana* 16c RSS assay

The *N*, *P*, *MP*, *M* and *G* genes carrying a stop codon and the cutting sites described above were inserted into the expression cassette (plasmid pSK, Leastro, Pallas [51]), under the control of the 35S promoter from cauliflower mosaic virus (CaMV) and the terminator from the potato proteinase inhibitor (PoPit). The resulting cassettes, 35S-*N*-PoPit, 35S-*P*-PoPit, 35S-*MP*-PoPit, 35S-*M*-PoPit and 35S-*G*-PoPit, were transferred to the pMOG800 binary plasmid using the *Hind*III restriction site. pMOG carrying HCPro and potato virus X p25 (a VSR that prevents the spread of RNA silencing signal), described previously [33], were used as controls. The introduction of the HA epitope at the C-terminus of the OFV proteins for protein detection was performed as previously described [19]. For all constructs assayed in this work, the correct gene insertion was confirmed by the Sanger sequencing method.

To test local RSS activity, leaves of the *N. benthamiana* 16 c line (six-leaf growth stage) [11, 16] were co-infiltrated with a mixture in equal volumes (OD_{600}=0.5) of *A. tumefaciens* strain C58C1 cultures transformed with pMOG800 harbouring eGFP (35S-GFP) and individual cultures carrying each of the aforementioned OFV genes. pMOG empty was used as control. The pMOG-35S-GFP construct carrying the eGFP gene was used to trigger the silencing of the GFP transgene of 16 c tobacco plants or to generate small RNAs (siRNAs) [19]. Three independent experiments were performed, each one including the infiltration of three plants per construct. The infiltrated leaves were photographed at 6 days p.i. under long-wavelength UV light (UVGL-58 Handheld UV lamp; UV Products) by using an iPhone XR camera with a 12-megapixel sensor, a six-element glass lens and an aperture of f/1.8 (Apple, Inc., Cupertino, CA, USA).

For systemic silencing analysis, 16 c leaves were co-infiltrated as a mixture of C58C1 cultures transformed with pMOG-35S-GFP and pMOG-35S-p25 (PVX p25, positive control), or pMOG empty (negative control) or pMOG-35S-MP, as mentioned above. Two independent experiments were performed, the first one using 10 plants, followed by 9 plants in the second assay. For combination 35S-GFP plus 35 S-p25, the spread of the systemic GFP silencing signal was analysed using nine 16 c plants. Plants were photographed at 16 days p.i. and the red fluorescence that indicates systemic silencing was monitored for up 30 days p.i. At 10 days p.i., images of the GFP expression surrounding the agroinfiltrated patches were taken to examine the cell-to-cell spread of the silencing signal.

RNA extraction and Northern blot analysis

Total RNAs from WT *N. benthamiana* leaves expressing the OFV proteins and controls in combination with PVX (at 4 and 14 days p.i.) and TCV (at 5 days p.i.) systems were extracted using VWR Life Science AMRESCO RiboZol RNA Extraction Reagent. Total RNA extractions were also performed from P12 protoplasts (at 16 h p.i.) and from 16 c plants (at 4 days p.i.). For the analyses of RNA accumulations of the AMV, PVX, TCV, siRNAs and mGFP RNAs by Northern blot technique, all procedures of RNA electrophoresis, membrane transference, hybridization and detection were conducted as previously described [19, 52]. For the detection of AMV and TCV genomic (g) and subgenomic (sg) RNAs, we used a DIG-riboprobe (Roche, Mannheim, Germany) complementary to their 3′UTR regions. For detection of genomic and subgenomic PVX RNAs, we used a 500 nt length (DIG)-labelled riboprobe complementary to the 3′ end region of the PVX CP gene. A 50 nt DIG-riboprobe complementary to nucleotides 707–756, 761–810 and 881–930 of the GFP gene was used for the detection of siRNAs. For the detection of mGFP RNA, a DIG-riboprobe complementary to the complete sequence of the GFP gene was used.

Statistical analysis

Statistical differences were examined using the Student's *t*-test. Comparisons were performed between the controls and viral factors (samples). Significant differences correspond to values of $P<0.05$. Values of P lower than 0.05 ($P<0.05$) are indicated by P^*, while values lower than 0.01 ($P<0.01$) are indicated by P^{**}. P^{NS} indicates no significant difference. RNA accumulations from Northern blot analyses are presented in bar graphs. Error bars represent the standard deviations (±SD) from the mean of three independent experiments with at least three replicates for each sample. We quantified the RNA bands using ImageJ version 2.0cr software with the ISAC plugin.

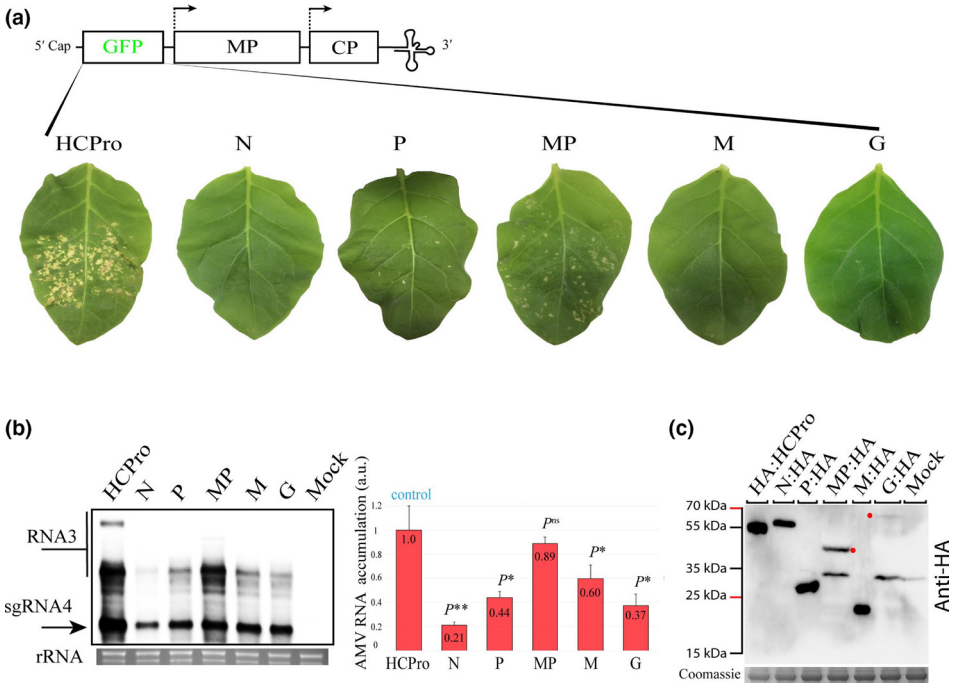

Fig. 1. The MP triggers necrotic response in P12 *Nicotiana tabacum* leaves. (a) Inoculation of transgenic P12 leaves with the alfalfa mosaic virus (AMV) RNA 3 derivative in which its green fluorescent gene (GFP) was exchanged by the tobacco etch virus HCPro and orchid fleck virus (OFV-citrus) genes (N, P, MP, M and G). The schematic representation shows the GFP/MP/CP AMV RNA 3 construct, in which the open reading frames corresponding to the GFP, the movement protein (MP) and the coat protein (CP) are represented by large boxes. Arrows represent subgenomic promoters. The 5′ and 3′ termini have Cap and tRNA-like (TLS) structures, respectively. The necrotic response is observed in leaves inoculated with AMV RNA 3 construct expressing the HCPro (positive control) and MP at 4 days post-inoculation (p.i.). Three independent experiments were performed, each one including the inoculation of three plants per construct. (b) Northern blot showing total accumulation of AMV RNAs in P12 protoplasts at 16 h post-inoculation, using a DIG-riboprobe complementary to the 3′UTR of the AMV. Transcripts correspond to the AMV RNA 3 derivative carrying the N, P, MP, M and G proteins of OFV-citrus and HCPro protein (control). Mock corresponds to the non-infected P12 protoplasts. rRNA stained with ethidium bromide indicates equal loading of samples. The localization of RNA 3 and subgenomic RNAs (sgRNA) is indicated. The graph represents the relative accumulation of total AMV RNAs, referring to the construct expressing the HCPro, from the average of three independent experiments [see all blots in panel (a) Fig. S2a]. The bands were quantified using ImageJ version 2.0cr software with the ISAC plugin and error bars represent the standard deviation. Statistical analysis was performed using Student's *t*-test. Asterisks (*) indicate significantly increased viral accumulation compared to the control. P^*, $P<0.05$; P^{**}, $P<0.01$; P^{ns}, no significant difference. *P*-values were obtained from pairwise comparisons between control vs viral factors. (c) Western blot analysis of the accumulation of proteins carrying the HA epitope in P12 leaves at 3 days p.i. The estimated sizes of OFV-citrus proteins, disregarding the fusion with HA epitope, are: N, ~49.3 kDa; P, ~26.4 kDa; MP, ~41.6 kDa; M, ~20 kDa; G, ~61.5 kDa. Red dots indicate the corresponding band for MP and G proteins. Unexpected bands for MP and G are visualized. Proteins stained with Coomassie blue indicate equal loading of samples.

RESULTS

The *cis* expression of OFV-citrus MP using the AMV system enhances vRNA and generates necrotic lesions on transgenic tobacco leaves

P12 tobacco leaves generate necrotic lesions when infected with AMV RNA 3 clones carrying a viral protein with RSS activity [18]. To test whether any of the OFV-citrus proteins are capable of modifying the AMV pathogenicity, the N, P, MP, M and G genes were cloned into the AMV RNA 3 by exchange of the GFP gene (Fig. 1a). Transcripts generated from AMV RNA 3 chimeric constructs were inoculated onto P12 tobacco leaves. The transgenic P12 plants constitutively express the replicase (P1 and P2) of AMV [42]. The lesions on the P12 leaves were monitored on the inoculated leaves for 1 week. Among all OFV-citrus proteins tested, MP expression generated a large number of necrotic lesions (at 4 days p.i.) on P12 leaves, similar to those observed by the expression of the helper component proteinase (HCPro) (positive control) (Fig. 1a), a well-characterized VSR [53]. No necrotic lesions were visualized in P12 leaves inoculated with AMV RNA 3 transcripts expressing the N, M and G proteins, whereas for the P protein very few were observed (Fig. 1a). The absence of necrotic lesions was also observed in P12 leaves inoculated with AMV RNA 3 WT construct (data not shown). No extra symptoms were observed over the 4 weeks in the upper leaves.

In order to confirm the expression and stability of the corresponding proteins, extraction of total proteins was performed from leaves inoculated with AMV transcripts carrying the heterologous genes at 3 days p.i., All proteins were detected using a monoclonal Anti-HA antibody (Fig. 1c).

The presence of an RSS in AMV RNA 3 increases the AMV accumulation in P12 protoplasts [18]. To investigate whether MP or other OFV candidate proteins are able to increase AMV accumulation, we transfected P12 protoplasts with the chimeric AMV RNA 3 constructs carrying the OFV-citrus genes. Northern blot analysis revealed that RNA 3 derivative expressing the MP increased the AMV RNA accumulation at comparable levels of HCPro (Fig. 1b). No significant differences in RNA accumulation were observed between HCPro and MP (*P*-values >0.05) (Fig. 1b, graph). On the other hand, equivalent levels of AMV RNA accumulation were not observed between the constructs expressing the N, P, M, and G with HCPro (Fig. 1b). This result indicates that MP has an RSS activity, as revealed by the AMV system in the P12 leaf context.

MP enhances the pathogenicity of the PVX infectious clone

The increase in the severity of the PVX infection suggests the presence of an additional gene with RSS activity [9]. To further test the RSS activity of MP, we cloned this gene into a pGR106 PVX construct (Fig. 2a) [44] and the symptomatology in the upper *N. benthamiana* leaves was monitored for 30 days. PVX constructs harbouring the HCPro gene (PVX-HCPro) and an empty PVX derivative were used as positive and negative controls, respectively.

We first agroinfiltrated *N. benthamiana* plants. Next, at 3 days p.i. and with the aim of mitigating the effect of agrobacterium in the PVX infection context, the infiltrated leaf was crushed in phosphate buffer and the leaf extract was used as virus particle inoculum to infect new *N. benthamiana* plants. At 4 days p.i., typical PVX symptoms (mosaic, mottling and interveinal chlorosis) were visualized in the mechanically inoculated plants expressing the constructs described above. At 10 days p.i., PVX-HCPro-infected plants developed severe symptoms that resulted in plant deaths at 30 days p.i. (Fig. 2b). PVX-MP-infected plants showed a strong mosaic symptom with the presence of necrotic punctate lesions dispersed throughout the upper leaves (data not shown), which developed into severe symptoms, generating plant deaths at 30 days p.i. (Fig. 2b). For plants infected with PVX-empty, the symptoms developed into a smooth mosaic (19 days p.i.) (Fig. 2b).

To correlate disease severity with PVX viral accumulation, we performed Northern blot analyses at 14 days p.i. (upper leaves). The quantification of genomic and subgenomic PVX RNAs revealed that the accumulation of viral RNAs increased more in those plants infected with PVX expressing the HCPro or OFV-citrus MP when compared with the empty PVX construct (Fig. 2c). The quantification of the PVX RNAs accumulation revealed that the PVX-MP and PVX HCPro accumulate approximately five (17.5 vs 3.25) and three (12.7 vs 3.25) times more vRNA than the empty PVX, respectively (Fig. 2c). These results indicate that MP significantly enhanced the pathogenicity of PVX by increasing virus accumulation.

To confirm the stability of the inserts, RT-PCR was performed using PVX primers flanking the region of gene insertion in the plasmid on total RNA extracted from upper non-infiltrated leaf early in infection (4 days p.i.). Expected MP and HCPro amplicon in upper non-inoculated leaves were visualized, indicating genetic stability (Fig. 2d). As expected, the PVX-empty amplicon corresponding to the region flanking the multiple clone sites of the vector was visualized (Fig. 2d).

OFV-citrus MP protein does not complement the RSS-defective turnip crinkle virus

The TCV system is a powerful tool to identify RSS activity for viral suppressors that act in local silencing [17]. We investigated the RSS activity of OFV-citrus MP using two approaches related to a movement-defective TCV system. The first one is based on the functional complementation of a movement-defective TCV clone (Fig. S3) (TCV-sGFP complementation assay) and in the second approach the presence of RSS activity is associated with an increase of the GFP signal derived from the binary pZP-TCV-sGFP construct (Fig. S3) (pZP-TCV-sGFP complementation assay) [17].

For the TCV-sGFP complementation assay, transcripts of movement-defective TCV-sGFP were mechanically inoculated in leaves of *N. benthamiana* previously infiltrated with binary constructs carrying the OFV-citrus MP, HCPro (positive control), or an empty pMOG vector (negative control). At 3 days p.i., the foci infection area, which indicates movement *trans*-complementation of the movement-defective TCV-sGFP, was visualized by the expression of RSS HCPro (Fig. S3b, complementation assay). On the other hand, the MP was not able to *trans*-complement the TCV-sGFP movement, revealing a GFP fluorescence signal distributed in individual cells on *N. benthamiana* leaves (Fig. S3b). As expected, pMOG-empty did not *trans*-complement the TCV-sGFP movement, only showing GFP signal in individual cells (Fig. S3b).

For the pZP/TCV-sGFP co-infiltration assay, leaves of *N. benthamiana* were co-agroinfiltrated with individual cultures transformed with pZP/TCV-sGFP vector and pMOG binary constructs (HCPro, OFV-citrus MP or empty). Leaves expressing the pMOG empty (negative control) and pMOG carrying the MP did not generate a visual increase of the GFP signal, in contrast to the GFP signal visualized by expression of the RSS HCPro (Fig. S3b, co-infiltration assay). Northern blotting revealed a significant increase of the TCV RNA accumulation in leaves expressing HCPro (Fig. S3c). Statistical significance in TCV RNA accumulation was not observed for the leaves expressing MP when compared to the negative control (Fig. S3c, graph).

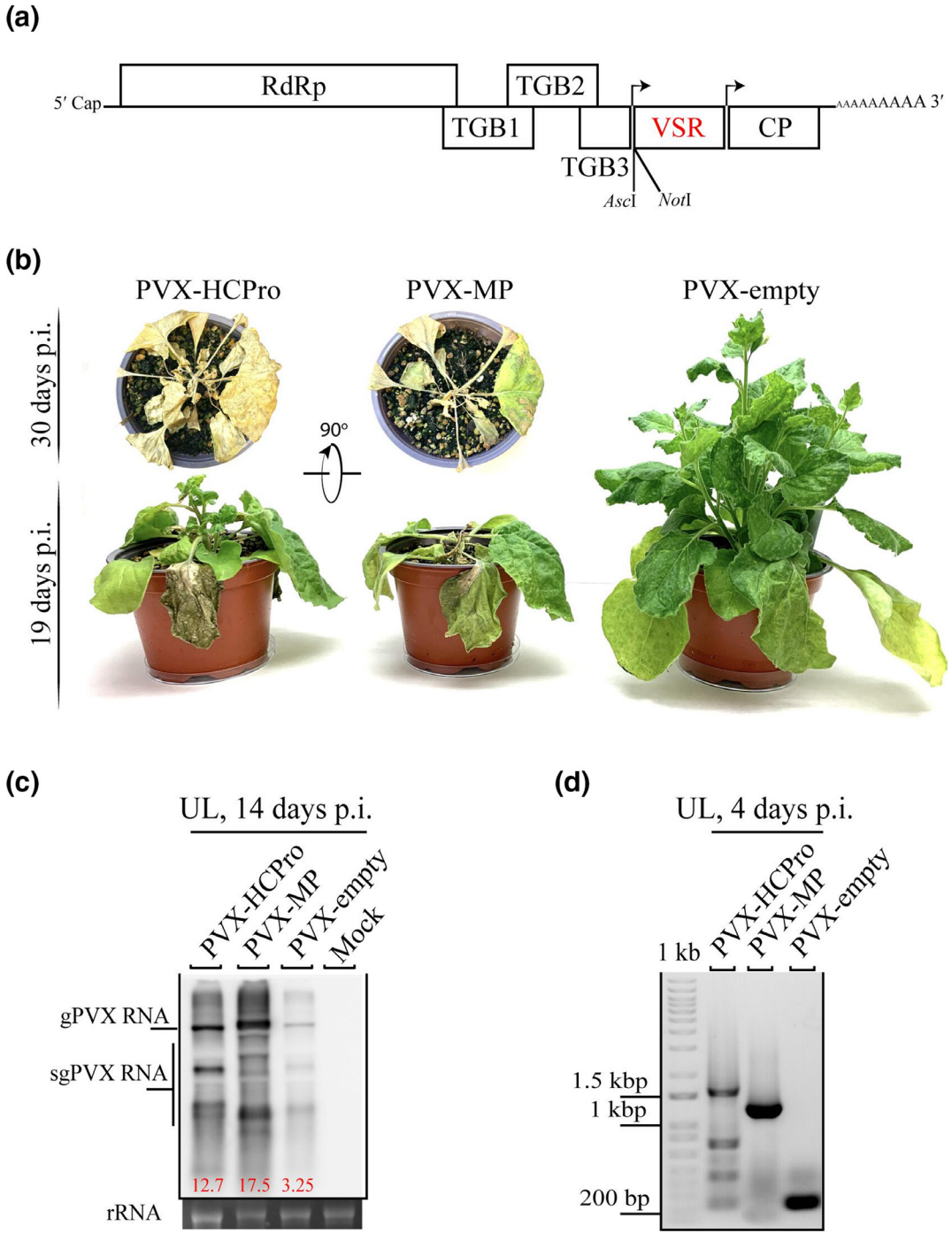

Fig. 2. RSS activity of OFV-citrus MP using the potato virus X (PVX) assay. (a) The schematic representation corresponds to the pGR106 PVX infectious construct carrying the *Asc*I and *Not*I restriction sites used for heterologous gene insertion downstream of the duplicated PVX CP promoter (arrow). RdRp, polymerase; TGB1-3, triple gene block; VSR, viral suppressor of RNA silencing; CP, coat protein. (b) Symptom phenotype of wild-type PVX (negative control) and PVX expressing the HCPro and OFV-citrus MP in *N. benthamiana* plants at 19 and 30 days p.i., (c) Northern blot analysis showing accumulation of the PVX RNAs at 14 days p.i. in upper leaves (ULs) using a DIG-riboprobe complementary to the 3' end region of the PVX CP gene. rRNA stained with ethidium bromide indicates equal loading of samples. Mock corresponds to an uninfected plant. Values of band quantification using the Image J version 2.0cr program are shown. (d) At 4 days p.i., RT-PCR analysis was performed to detect the HCPro and MP genes in symptomatic upper leaves of *N. benthamiana* plants inoculated with pGR107-HCPro and pGR106-MP constructs. The marker DNA band sizes from 200 to 1500 base pairs (bp) are indicated. PVX empty (258 bp), PVX-HCPro (1.377 +258 bp) and PVX-MP (1.113 +258 bp) amplicons were generated by using PVX primers flanking the insertion gene region.

OFV-citrus proteins failed to suppress the local GFP silencing in *N. benthamiana* 16 c

In the 16 c system, the transient expression of an RSS blocks the locally induced silencing triggered by the GFP, allowing the visualization of a bright green signal derived from the transiently expressed GFP for periods longer than 6 days. If the candidate protein has no RSS activity, the infiltrated region emits a signal to silence the GFP that spreads to distal regions in the plant through the phloem [15]. To determine the putative local RSS activity of the OFV-citrus proteins, 16 c plant leaves were co-agroinfiltrated with individual cultures transformed with pMOG-35S-GFP (35S-GFP) – as an inductor for gene silencing – and pMOG constructs harbouring OFV-citrus genes (35S-N, 35S-P, 35S-MP, 35S-M and 35S-G). Empty pMOG vector or carrying the HCPro were used as negative and positive controls, respectively. At 6 days p.i., leaves of *N. benthamiana* 16 c infiltrated with the 35S-GFP plus empty construct showed a red patch in the infiltrated area under UV light, indicating local GFP silencing (Fig. 3a). A similar phenotype was visualized in all leaves co-infiltrated with 35S-GFP plus pMOGs carrying the N, P, MP, M and G OFV genes (Fig. 3a). In contrast, the 16 c leaves expressing HCPro maintained a high level of GFP signal (Fig. 3a). To confirm the expression of the corresponding proteins, extraction of total proteins from leaves infiltrated with pMOG vectors carrying the OFV genes was performed at 5 days p.i. All proteins were detected using an Anti-HA monoclonal antibody (Fig. 3b).

Northern blot analysis of the GFP mRNA accumulation at 4 days p.i. reaffirmed the visual results of the GFP signal. No statistical significance in GFP mRNA accumulation was identified for the leaves expressing the OFV-citrus proteins when compared to the negative control, but a significant difference in GFP mRNA accumulation was observed in a comparison between leaves expressing HCPro and the negative control (Fig. 3c, graph).

To evaluate a possible RSS activity mediated by at least two viral proteins, different combinations (N+P, N+MP, N+M, N+G, P+MP, P+M, P+G, MP +M, MP +G, M+G and N+P+MP+M+G) of the five OFV proteins were co-expressed with the GFP inducer. No increment of the GFP signal was visualized at 4 days p.i. in any combination performed (Fig. S4).

MP expression alters the accumulation of the siRNA GFP in 16 c plants

VSRs may regulate the production or activity of short interfering RNAs (siRNAs) and micro-RNAs (miRNAs) [19, 53, 54]. In this regard, we examined whether the MP that showed RSS activity using viral systems could interfere with the siRNA accumulation in 16 c leaves. Northern blot analysis of GFP siRNA accumulation in infiltrated 16 c leaves co-expressing the 35S-GFP plus N, MP, HCPro, or empty pMOG vector at 4 days p.i. revealed that the expression of the MP significantly reduced the accumulation level of the GFP siRNAs, similar to what had been observed for the HCPro (Fig. 3d). No differences were observed between the leaves infiltrated with the empty pMOG vector (negative control) or the N protein (control used for comparison of the MP with other OFV protein). This result further indicates that MP may act as a viral suppressor of RNA silencing.

MP could prevent the systemic silencing, but not the cell-to-cell movement of the silencing signal

MP failed in the TCV analysis – a viral system that is limited to identifying viral factors with systemic RSS activity – but it showed RSS activity when using the AMV and PVX approaches. This points to a link between MP suppressor activity with possible prevention of systemic silencing. In this sense, we decided to investigate whether MP is able to block the cell-to-cell and long-distance spread of the silencing signal using the 16 c plants. To investigate whether the MP can inhibit the intercellular traffic of the silencing signal, we monitored the presence or not of a red patch at the edge of the infiltrated regions in the leaves of 16 c plants. As described by Yang *et al.* [55], in this system, the movement of the silencing signal from the agroinfiltrated area causes a strong reduction of GFP transgene expression in a zone of 10 to 15 adjacent cells, which can be visualized under UV light as a characteristic red ring around the infiltration area [56]. At 10 days p.i., an obvious red ring was observed in 16 c leaves co-expressing the 35S-GFP and OFV-citrus 35S-MP, similar to that visualized in leaves expressing 35S-GFP and empty pMOG vector (negative control) (Fig. 4a). As expected, leaves expressing the PVX p25, which was previously identified as a VSR acting in steps of systemic silencing, did not develop a red ring around the infiltrated zone (Fig. 4a). This finding suggests that MP has no ability to inhibit the short-range (cell-to-cell) spread of RNA silencing.

The silencing signal can travel over long distances through the phloem [57]. Systemic GFP silencing is visually indicated by the presence of a red fluorescence distributed throughout the plant. To assess whether MP affects this process, GFP fluorescence was monitored in newly upper leaves of 16 c plants infiltrated with 35S-GFP and 35S-MP or 35S-GFP and 35 S-p25 or 35S-GFP and empty pMOG vector. At 16 days p.i., in the plants infiltrated with 35S-GFP and pMOG empty, red fluorescence was visualized in upper non-infiltrated leaves, indicating systemic silencing. Ten out of 19 plants showed red fluorescence, a suppression efficiency of 47.3% (Fig. 4b, table). In contrast, the plants infiltrated with 35S-GFP plus 35 S-p25 (positive control) or 35S-MP maintained GFP fluorescence with a suppression efficiency of 100% (Fig. 4b). Taken together, these findings indicate that MP may be able to inhibit long-distance spread but does not block short cell-to-cell spread of RNA silencing signal.

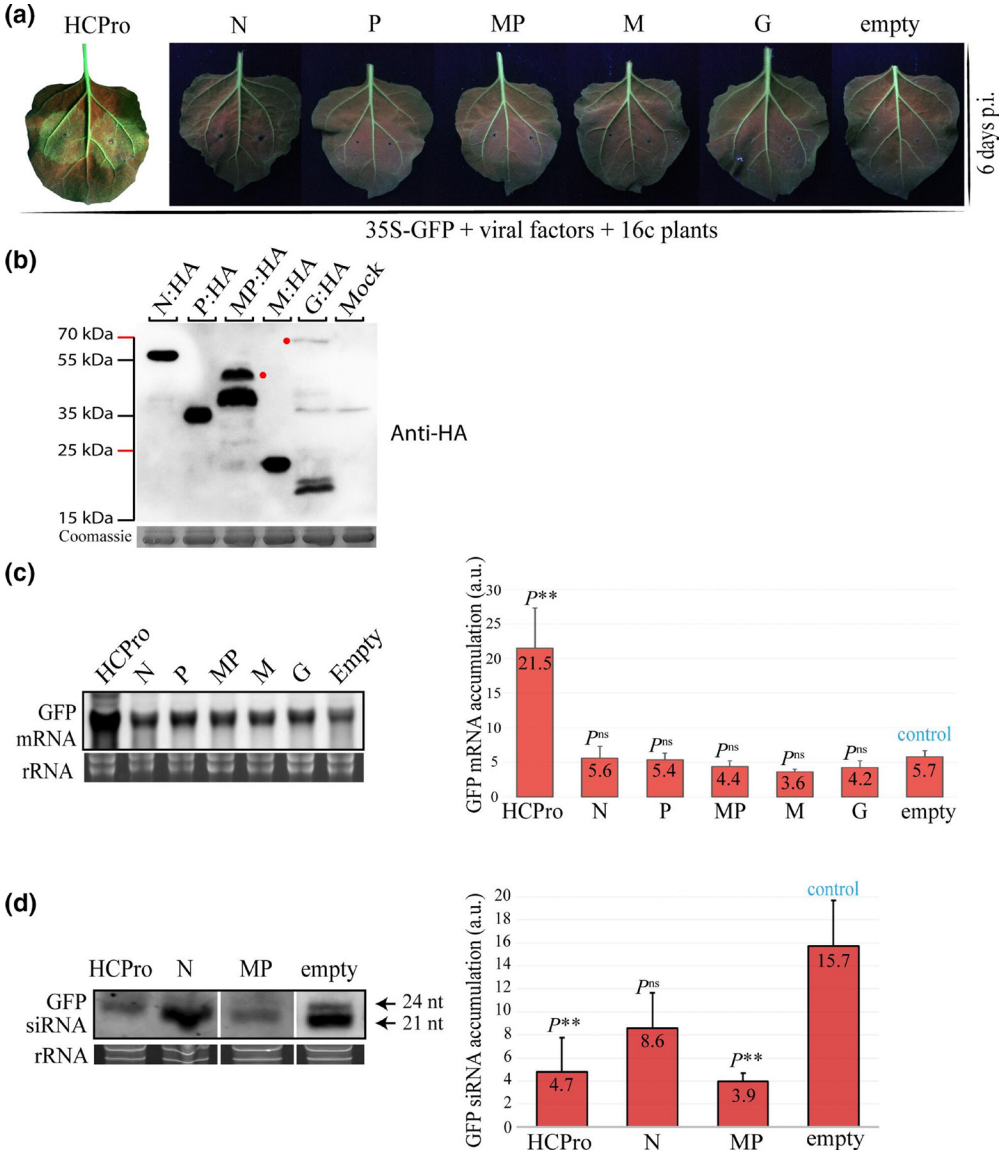

Fig. 3. Transient expression of OFV-citrus encoded proteins in *Nicotiana benthamiana* 16c plants. (a) Fluorescent images of *N. benthamiana* 16c leaves co-infiltrated with agrobacterium suspension carrying pMOG binary construct presented in panel (a) containing individual OFV-citrus ORFs and the eGFP that was used to trigger the silencing of the GFP transgene. The ORFs were cloned between CaMV 35S promoter and potato proteinase inhibitor terminator (PoPit). Agrobacterium cultures carrying the binary pMOG-HCPro or the empty pMOG constructs were co-infiltrated with the culture expressing GFP (pMOG-GFP) as positive and negative controls, respectively. GFP fluorescence was not observed in leaves expressing the five OFV-citrus proteins at 6 days post-infiltration. Three independent experiments were performed, each one including the infiltration of three plants per construct. (b) Western blot analysis of the accumulation of proteins carrying the HA epitope in *N. benthamiana* leaves at 5 days p.i. The estimated sizes of OFV-citrus proteins, disregarding the fusion with HA epitope are: N, ~49.3 kDa; P, ~26.4 kDa; MP, ~41.6 kDa; M, ~20 kDa; G, ~61.5 kDa. Red dots indicate the corresponding band for MP and G proteins. Unexpected bands for MP and G are visualized. Proteins stained with Coomassie blue indicate equal loading of samples. (c) Northern blot analysis of GFP mRNA extracted at 4 days p.i. from the leaves infiltrated with the combination constructs referred to above was performed using a DIG-riboprobe complementary to the GFP gene. rRNA stained with ethidium bromide indicates equal loading of samples. The graph represents the accumulation of mGFP RNAs corresponding to the average of three Northern blots from three independent experiments (see all blots in Fig. S2b). The bands were quantified using ImageJ version 2.0cr software with the ISAC plugin and error bars represent the standard deviation. Statistical analysis was performed using Student's *t*-test. Asterisks (*) indicate significantly increased viral accumulation compared to the control. P^{**}, $P<0.01$; P^{ns}, no significant difference. *P*-values were obtained from pairwise comparisons between control vs viral factors. (d) Northern blot of GFP-specific siRNA extracted from *N. benthamiana* 16c patches at 4 days p.i. co-infiltrated with constructs expressing the GFP plus constructs expressing the HCPro (positive control), N and MP OFV-citrus proteins. Membranes were hybridized using a mix of three 50 nt riboprobes complementary to the GFP gene. Negative control (empty) corresponds to patches co-infiltrated with agrobacterium cultures carrying the GFP construct and the empty binary plasmid. Small RNAs of 21 and 24 nt are indicated. rRNA stained with ethidium bromide indicates equal loading of samples. The graph represents the accumulation of GFP siRNA from three independent experiments (see all blots in Fig. S2c). Error bars represent the standard deviation. Statistical analyses were performed using Student's *t*-test. Asterisks (*) indicate significantly decreased viral accumulation compared to the control. P^{**}, $P<0.01$; P^{ns}, no significant difference.

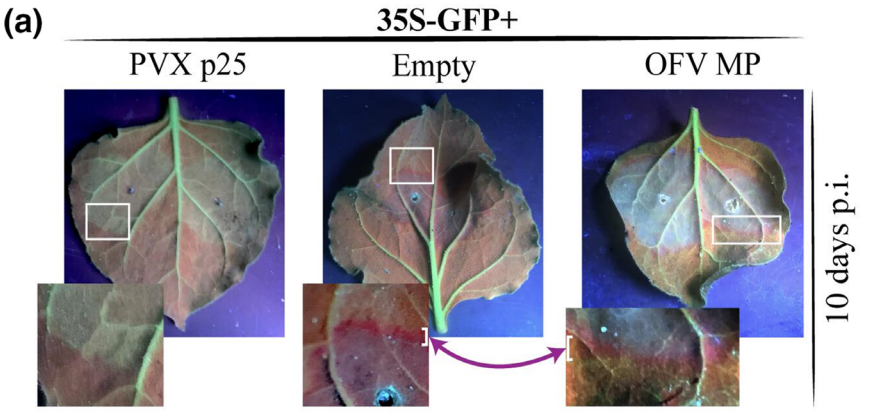

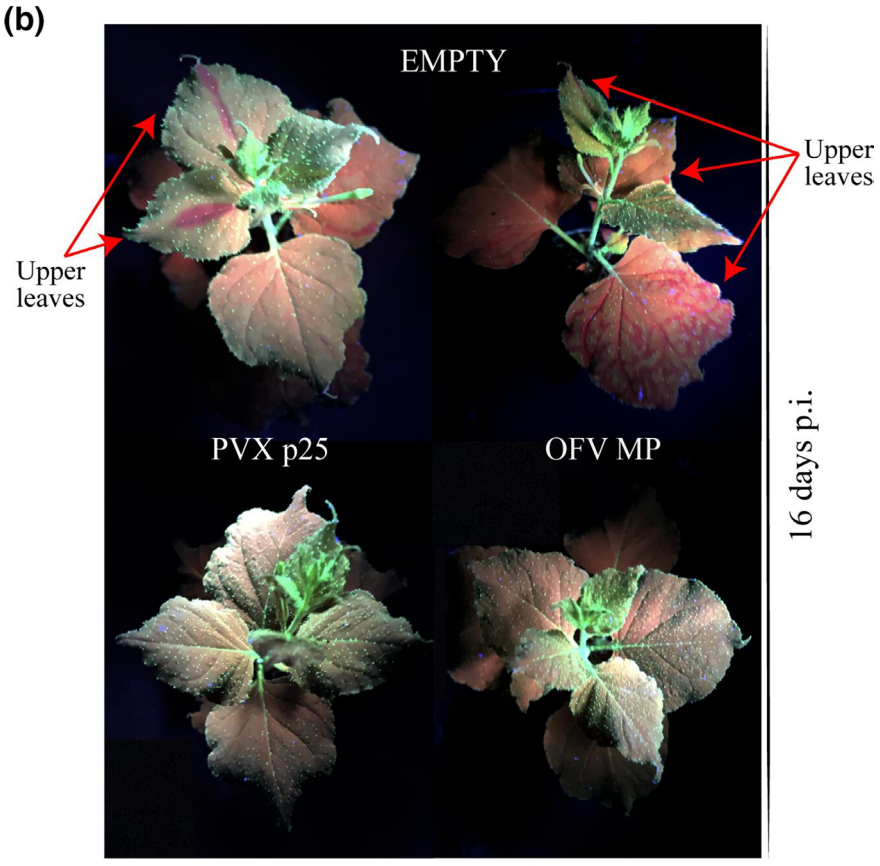

Construct pMOG 35S-GFP +	No. plants infiltrated	No. plants systemically silenced	Suppression efficiency (%)
pMOG 35S-empty	19	10	47.3
pMOG 35S-p25	9	0	100
pMOG 35S-MP	19	0	100

Fig. 4. Effect of OFV-citrus MP on the short- and long-distance spread of systemic silencing GFP in *N. benthamiana* 16 c plants. (a) Fluorescent leaf images at 10 days p.i. expressing the 35S-GFP in combination with 35S-p25PVX (positive control), 35S-MP (OFV-citrus) and empty pMOG vector (negative control). The double-headed purple arrow together with white brackets points to red rings around the infiltrated zone. (b) Fluorescent images of *N. benthamiana* 16 c plants at 16 days p.i. expressing the protein combinations mentioned in panel (a). Red arrows indicate the silencing signal in upper non-infiltrated leaves. The table shows the numbers of infiltrated *N. benthamiana* 16 c plants systemically silenced and the percentage of suppression efficiency.

DISCUSSION

Movement proteins play an essential role in the viral infection cycle by ensuring the intercellular spread of viral components or particles from the initial infected cell to the neighbouring cells and upper regions of the plant through the plasmodesmata and the vascular tissue [58, 59]. Furthermore, MPs may act in other important steps of the viral infection cycle. Currently, several studies have shown a role for MPs in suppressing the RNA silencing machinery [15, 23, 38, 60, 61]. A comprehensive study on the functionality of the dichorhaviruses MP suggests that this protein might guide the intracellular trafficking of the viral components and may be associated with the cell-to-cell movement mechanism of dichorhaviruses [33]. Here, we increased our knowledge concerning the functionality of the OFV-citrus MP. First using viral systems (AMV, PVX and TCV), and then the 16 c 'patch' technique for the analyses of local (GFP mRNA and siRNA accumulation), cell-to-cell (short-range spread of RNA silencing), and systemic (long-distance spread of silencing signal) GFP silencing, we evaluated the potential RSS activity for the OFV-citrus MP. The AMV and PVX systems clearly showed that the OFV-citrus MP protein is a strong viral suppressor of RNA silencing. To discern whether this activity operated at a local or systemic level, assays to complement the movement-defective TCV-sGFP constructs or to record GFP fluorescence in 16 c plants were carried out.

In the analysis of GFP mRNA expression (16 c system), MP and other OFV-citrus candidate proteins were unable to suppress local silencing. However, in the case of MP, the accumulation level of the GFP-derived siRNAs was significantly reduced, indicating that this protein probably targets upstream step(s) of dsRNA production. Similar RSS activity was observed with part of the proteins encoded by citrus leprosis virus C (CiLV-C), the type species of the genus *Cilevirus*, which converges evolutionarily with dichorhaviruses. Thus, three CiLV-C proteins (p15, p29 and p61) were identified as VSRs, allowing the reduction of the accumulation level of the GFP-derived siRNAs, but they were unable to suppress GFP overexpression in the infiltrated tissue [19]. An inverse correlation has been reported for the P protein of another member of the family *Rhabdoviridae*, the lettuce necrotic yellows cytorhabdovirus (LNYV). LNVY P protein acts as a local RSS but does not prevent GFP siRNA accumulation in *N. benthamiana* [36]. As proposed for LNVY P, the mode of action of OFV-citrus MP and RSS CiLV-C proteins could also be unlike those of the majority of viral RSS, which sequester small RNAs. These expressive divergences in the mechanism of action among different VSRs further reinforce the idea that a constant co-evolution between pathogens and organisms gives rise to a large variety of defence pathways and counter-acting virulence pathways.

MP was indeed unable to maintain increased GFP expression in infiltrated tissue for periods longer than 6 days, suggesting that it does not act as a local silencing suppressor, but given the ability of MP to block GFP siRNA production, we cannot exclude that this protein could act as a transient local VSR, showing weak suppressor activity. The hypothesis of weak local RSS activity for MP is further reinforced by the local suppressor activity observed for it in the P12 protoplasts (AMV system). Viral proteins with weak or no local suppressor activity have been constantly observed in several characterized viral suppressors [15, 37, 61–63].

Using a sensitive method to screen for RSS activity based on AMV RNA 3 derivative [18], we identified clear enhancement of AMV pathogenicity from *cis* expression of the OFV-citrus MP, indicating suppressor activity for this protein. This method has been applied to assist the characterization of VSRs. The CP of carnation mottle virus (CarMV), 2b of cucumber mosaic virus (CMV), HCPro of TEV, p19 of tomato bushy stunt virus (TBSV), and p15, p29 and p61 of CiLV-C are some examples of proteins assayed in this system that showed RSS activity, as well as in other well-characterized systems for RSS screening [18, 19].

Several VSR proteins enhanced the severity of PVX infection, a phenotype well known to be associated with RSS activity [15, 19, 22, 55, 64]. The PVX-MP infection resulted in severe viral symptoms and increased vRNA accumulation, resulting in the death of tobacco wild plants when compared to the control (PVX-empty). Enhancement of PVX virulence also has been described for the P6 of rice yellow stunt alphanucleorhabdovirus (RYSV), another member of the family *Rhabdoviridae* [37]. In addition to the enhancement of classical mosaic symptoms of PVX infection, the presence of small punctate necrotic lesions was noted in the upper leaves infected with PVX-MP, suggesting activation of programmed cell death (PCD). These systemic lesions were very similar to the phenotype of systemic necrosis associated with PCD observed from infection of PVX expressing the broad bean wilt virus 1 (BBWV-1) VP37 protein, which has a role in virus pathogenicity, host specificity and suppression of post-transcriptional gene silencing (PTGS) [64]. Investigating the upregulation of plant genes related to the production of toxic ROS (reactive oxygen species) from OFV-citrus MP expression should be a next step to confirm PCD and assess the potential role of this MP as a viral determinant of pathogenicity.

A TCV complementation test failed to identify RSS activity for the triple gene block 1 (TGB-p25) of PVX, which acts by blocking systemic silencing but is incapable of suppressing local silencing of replicating transgenes [15, 17]. A similar result was observed here for the expression of the OFV-citrus MP, which was unable to rescue TCV-sGFP movement and increase the sGFP signal. This points to the observation that, like the PVX p25, the OFV-citrus MP may more expressively affect the RNAi pathway at the systemic level, which was confirmed by the analysis with 16 c plants.

Although OFV-citrus MP could not prevent the short-distance spread of the silencing signal, it could interfere with the systemic long-distance spread. Similar behaviour has been reported for the V2 protein of mulberry mosaic dwarf-associated geminivirus (MMDaV) and the P protein of alfalfa dwarf cytorhabdovirus (ADV) [35, 55]. To unravel the mechanisms of suppression of RNA

silencing by OFV MP, it would be interesting to investigate whether MP suppresses systemic PTGS, impairing the RNA-dependent RNA polymerase 6 (RDR6) or co-factors, as a suppressor of gene silencing 3 (SGS3), implicated in the genesis of secondary siRNA [65–68]. Suppression of the PTGS, impairing the RDR6/SGS3 pathway, has been reported for the P6 of RYSV, the P of ADV and LNYV, and the P and P3 (movement protein) of barley yellow striate mosaic cytorhabdovirus (BYSMV), a group of viruses evolutionary related to the dichorhaviruses [35, 37–39].

In summary, our data establish that a dichorhavirus MP exhibits RSS activity. Furthermore, our findings suggest that MP likely acts more efficiently in step(s) of the systemic silencing pathway to prevent the spread of the long-distance silencing signal.

Funding information
This work was supported by grant PID2020-115571RB-100 from the Spanish MCIN/AEI/10.13039/501100011033 granting agency and Fondo Europeo de Desarrollo Regional (FEDER), and by the company INVESTIR IMÓVEIS LDTA from Brasília, Brazil.

Acknowledgements
We are grateful to Lorena Corachán for her excellent technical support and to G. Otero Colina (Colegio de Postgraduados, Texcoco, Mexico) and J. Freitas-Astúa (Embrapa mandioca e fruticultura, Bahia, Brazil) for kindly providing the OFV-citrus sample used in this work.

Author contribution
Conceptualization, M.O.L.; formal analysis, M.O.L. and J.A.S.-N.; investigation, M.O.L.; project supervision, J.A.S.-N.; writing — original draft, M.O.L.; writing — review and editing, V.P. and J.A.S.-N.; funding acquisition, M.O.L., V.P. and J.A.S.-N. All authors have read and agreed to the published version of the manuscript.

Conflicts of interest
The authors declare that there are no conflicts of interest.

Ethical statement
This article does not contain any studies with human participants or animals requiring ethical approval.

References

1. Molnar A, Melnyk C, Baulcombe DC. Silencing signals in plants: a long journey for small RNAs. *Genome Biol* 2011;12:215.
2. Pumplin N, Voinnet O. RNA silencing suppression by plant pathogens: defence, counter-defence and counter-counter-defence. *Nat Rev Microbiol* 2013;11:745–760.
3. Hamilton AJ, Baulcombe DC. A species of small antisense RNA in posttranscriptional gene silencing in plants. *Science* 1999;286:950–952.
4. Hammond SM, Bernstein E, Beach D, Hannon GJ. An RNA-directed nuclease mediates post-transcriptional gene silencing in Drosophila cells. *Nature* 2000;404:293–296.
5. Borges F, Martienssen RA. The expanding world of small RNAs in plants. *Nat Rev Mol Cell Biol* 2015;16:727–741.
6. Takeda A, Iwasaki S, Watanabe T, Utsumi M, Watanabe Y. The mechanism selecting the guide strand from small RNA duplexes is different among argonaute proteins. *Plant Cell Physiol* 2008;49:493–500.
7. Ding SW, Voinnet O. Antiviral immunity directed by small RNAs. *Cell* 2007;130:413–426.
8. Nakanishi K. Anatomy of RISC: how do small RNAs and chaperones activate Argonaute proteins? *Wiley Interdiscip Rev RNA* 2016;7:637–660.
9. Voinnet O, Pinto YM, Baulcombe DC. Suppression of gene silencing: a general strategy used by diverse DNA and RNA viruses of plants. *Proc Natl Acad Sci U S A* 1999;96:14147–14152.
10. Moon JY, Park JM. Cross-talk in viral defense signaling in plants. *Front Microbiol* 2016;7:2068.
11. Burgyán J, Havelda Z. Viral suppressors of RNA silencing. *Trends Plant Sci* 2011;16:265–272.
12. Li WX, Ding SW. Viral suppressors of RNA silencing. *Curr Opin Biotechnol* 2001;12:150–154.
13. Lu R, Folimonov A, Shintaku M, Li W-X, Falk BW, *et al*. Three distinct suppressors of RNA silencing encoded by a 20-kb viral RNA genome. *Proc Natl Acad Sci U S A* 2004;101:15742–15747.
14. Mérai Z, Kerényi Z, Kertész S, Magna M, Lakatos L, *et al*. Double-stranded RNA binding may be a general plant RNA viral strategy to suppress RNA silencing. *J Virol* 2006;80:5747–5756.
15. Voinnet O, Lederer C, Baulcombe DC. A viral movement protein prevents spread of the gene silencing signal in Nicotiana benthamiana. *Cell* 2000;103:157–167.
16. Hamilton A, Voinnet O, Chappell L, Baulcombe D. Two classes of short interfering RNA in RNA silencing. *EMBO J* 2002;21:4671–4679.
17. Powers JG, Sit TL, Qu F, Morris TJ, Kim K-H, *et al*. A versatile assay for the identification of RNA silencing suppressors based on complementation of viral movement. *Mol Plant Microbe Interact* 2008;21:879–890.
18. Martínez-Pérez M, Navarro JA, Pallás V, Sánchez-Navarro JA. A sensitive and rapid RNA silencing suppressor activity assay based on alfalfa mosaic virus expression vector. *Virus Res* 2019;272:197733.
19. Leastro MO, Castro DYO, Freitas-Astúa J, Kitajima EW, Pallás V, *et al*. Citrus Leprosis Virus C Encodes Three Proteins With Gene Silencing Suppression Activity. *Front Microbiol* 2020;11:1231.
20. Moissiard G, Voinnet O. Viral suppression of RNA silencing in plants. *Mol Plant Pathol* 2004;5:71–82.
21. Voinnet O, Vain P, Angell S, Baulcombe DC. Systemic spread of sequence-specific transgene RNA degradation in plants is initiated by localized introduction of ectopic promoterless DNA. *Cell* 1998;95:177–187.
22. Cañizares MC, Navas-Castillo J, Moriones E. Multiple suppressors of RNA silencing encoded by both genomic RNAs of the crinivirus, Tomato chlorosis virus. *Virology* 2008;379:168–174.
23. Renovell Á, Vives MC, Ruiz-Ruiz S, Navarro L, Moreno P, *et al*. The Citrus leaf blotch virus movement protein acts as silencing suppressor. *Virus Genes* 2012;44:131–140.
24. Gupta AK, Hein GL, Graybosch RA, Tatineni S. Octapartite negative-sense RNA genome of High Plains wheat mosaic virus encodes two suppressors of RNA silencing. *Virology* 2018;518:152–162.
25. Samuel GH, Wiley MR, Badawi A, Adelman ZN, Myles KM. Yellow fever virus capsid protein is a potent suppressor of RNA silencing that binds double-stranded RNA. *Proc Natl Acad Sci U S A* 2016;113:13863–13868.
26. Freitas-Astúa J, Ramos-González PL, Arena GD, Tassi AD, Kitajima EW. Brevipalpus-transmitted viruses: parallelism beyond a common vector or convergent evolution of distantly related pathogens? *Curr Opin Virol* 2018;33:66–73.

27. Dietzgen RG, Freitas-Astúa J, Chabi-Jesus C, Ramos-González PL, Goodin MM, *et al*. Dichorhaviruses in their Host Plants and Mite Vectors. *Adv Virus Res* 2018;102:119–148.
28. Roy A, Stone AL, Shao J, Otero-Colina G, Wei G, *et al*. Identification and Molecular Characterization of Nuclear Citrus leprosis virus, a Member of the Proposed Dichorhavirus Genus Infecting Multiple Citrus Species in Mexico. *Phytopathology* 2015;105:564–575.
29. Cruz-Jaramillo JL, Ruiz-Medrano R, Rojas-Morales L, López-Buenfil JA, Morales-Galván O, *et al*. Characterization of a proposed dichorhavirus associated with the citrus leprosis disease and analysis of the host response. *Viruses* 2014;6:2602–2622.
30. Cook G, Kirkman W, Clase R, Steyn C, Basson E, *et al*. Orchid fleck virus associated with the first case of citrus leprosis-N in South Africa. *Eur J Plant Pathol* 2019;155:1373–1379.
31. Kondo H, Maruyama K, Chiba S, Andika IB, Suzuki N. Transcriptional mapping of the messenger and leader RNAs of orchid fleck virus, a bisegmented negative-strand RNA virus. *Virology* 2014;452–453:166–174.
32. Kondo H, Chiba S, Andika IB, Maruyama K, Tamada T, *et al*. Orchid fleck virus structural proteins N and P form intranuclear viroplasm-like structures in the absence of viral infection. *J Virol* 2013;87:7423–7434.
33. Leastro MO, Freitas-Astúa J, Kitajima EW, Pallás V, Sánchez-Navarro JA. Dichorhaviruses movement protein and nucleoprotein form a protein complex that may be required for virus spread and interacts in vivo with viral movement-related cilevirus proteins. *Front Microbiol* 2020;11:571807.
34. Dietzgen RG, Kuhn JH, Clawson AN, Freitas-Astúa J, Goodin MM, *et al*. Dichorhavirus: a proposed new genus for Brevipalpus mite-transmitted, nuclear, bacilliform, bipartite, negative-strand RNA plant viruses. *Arch Virol* 2014;159:607–619.
35. Bejerman N, Mann KS, Dietzgen RG. Alfalfa dwarf cytorhabdovirus P protein is a local and systemic RNA silencing supressor which inhibits programmed RISC activity and prevents transitive amplification of RNA silencing. *Virus Res* 2016;224:19–28.
36. Mann KS, Johnson KN, Dietzgen RG. Cytorhabdovirus phosphoprotein shows RNA silencing suppressor activity in plants, but not in insect cells. *Virology* 2015;476:413–418.
37. Guo H, Song X, Xie C, Huo Y, Zhang F, *et al*. Rice yellow stunt rhabdovirus protein 6 suppresses systemic RNA silencing by blocking RDR6-mediated secondary siRNA synthesis. *Mol Plant Microbe Interact* 2013;26:927–936.
38. Rabieifaradonbeh S, Afsharifar A, Finetti-Sialer MM. Molecular and functional characterization of the barley yellow striate mosaic virus genes encoding phosphoprotein, P3, P6 and P9. *Eur J Plant Pathol* 2021;161:107–121.
39. Mann KS, Johnson KN, Carroll BJ, Dietzgen RG. Cytorhabdovirus P protein suppresses RISC-mediated cleavage and RNA silencing amplification in planta. *Virology* 2016;490:27–40.
40. Ruiz MT, Voinnet O, Baulcombe DC. Initiation and maintenance of virus-induced gene silencing . *Plant Cell* 1998;10:937–946.
41. Patil BL, Fauquet CM. Light intensity and temperature affect systemic spread of silencing signal in transient agroinfiltration studies. *Mol Plant Pathol* 2015;16:484–494.
42. van Dun CM, van Vloten-Doting L, Bol JF. Expression of alfalfa mosaic virus cDNA1 and 2 in transgenic tobacco plants. *Virology* 1988;163:572–578.
43. Leastro MO, Freitas-Astúa J, Kitajima EW, Pallás V, Sánchez-Navarro JA. Unravelling the involvement of cilevirus p32 protein in the viral transport. *Sci Rep* 2021;11:2943.
44. Lu R, Malcuit I, Moffett P, Ruiz MT, Peart J, *et al*. High throughput virus-induced gene silencing implicates heat shock protein 90 in plant disease resistance. *EMBO J* 2003;22:5690–5699.
45. Sanchez-Navarro J, Miglino R, Ragozzino A, Bol JF. Engineering of alfalfa mosaic virus RNA 3 into an expression vector. *Arch Virol* 2001;146:923–939.
46. Leastro MO, Villar-Álvarez D, Freitas-Astúa J, Kitajima EW, Pallás V, *et al*. Spontaneous Mutation in the Movement Protein of Citrus Leprosis Virus C2, in a Heterologous Virus Infection Context, Increases Cell-to-Cell Transport and Generates Fitness Advantage. *Viruses* 2021;13:2498.
47. Taschner PE, van der Kuyl AC, Neeleman L, Bol JF. Replication of an incomplete alfalfa mosaic virus genome in plants transformed with viral replicase genes. *Virology* 1991;181:445–450.
48. Loesch-Fries LS, Jarvis NP, Krahn KJ, Nelson SE, Hall TC. Expression of alfalfa mosaic virus RNA 4 cDNA transcripts in vitro and in vivo. *Virology* 1985;146:177–187.
49. Jones L, Hamilton AJ, Voinnet O, Thomas CL, Maule AJ, *et al*. RNA-DNA interactions and DNA methylation in post-transcriptional gene silencing. *Plant Cell* 1999;11:2291–2301.
50. Hellens RP, Edwards EA, Leyland NR, Bean S, Mullineaux PM. pGreen: a versatile and flexible binary Ti vector for Agrobacterium-mediated plant transformation. *Plant Mol Biol* 2000;42:819–832.
51. Leastro MO, Pallás V, Resende RO, Sánchez-Navarro JA. The movement proteins (NSm) of distinct tospoviruses peripherally associate with cellular membranes and interact with homologous and heterologous NSm and nucleocapsid proteins. *Virology* 2015;478:39–49.
52. Pallás V, Más P, Sánchez-Navarro JA. Detection of plant RNA viruses by nonisotopic dot-blot hybridization. *Methods Mol Biol* 1998;81:461–468.
53. Anandalakshmi R, Pruss GJ, Ge X, Marathe R, Mallory AC, *et al*. A viral suppressor of gene silencing in plants. *Proc Natl Acad Sci U S A* 1998;95:13079–13084.
54. Mallory AC, Reinhart BJ, Bartel D, Vance VB, Bowman LH. A viral suppressor of RNA silencing differentially regulates the accumulation of short interfering RNAs and micro-RNAs in tobacco. *Proc Natl Acad Sci U S A* 2002;99:15228–15233.
55. Yang X, Ren Y, Sun S, Wang D, Zhang F, *et al*. Identification of the Potential Virulence Factors and RNA Silencing Suppressors of Mulberry Mosaic Dwarf-Associated Geminivirus. *Viruses* 2018;10:E472.
56. Himber C, Dunoyer P, Moissiard G, Ritzenthaler C, Voinnet O. Transitivity-dependent and -independent cell-to-cell movement of RNA silencing. *EMBO J* 2003;22:4523–4533.
57. Melnyk CW, Molnar A, Baulcombe DC. Intercellular and systemic movement of RNA silencing signals. *EMBO J* 2011;30:3553–3563.
58. Lucas WJ. Plant viral movement proteins: agents for cell-to-cell trafficking of viral genomes. *Virology* 2006;344:169–184.
59. Navarro JA, Sanchez-Navarro JA, Pallas V. Key checkpoints in the movement of plant viruses through the host. *Adv Virus Res* 2019;104:1–64.
60. Amari K, Vazquez F, Heinlein M. Manipulation of plant host susceptibility: an emerging role for viral movement proteins? *Front Plant Sci* 2012;3:10.
61. Fusaro AF, Barton DA, Nakasugi K, Jackson C, Kalischuk ML, *et al*. The Luteovirus P4 Movement Protein Is a Suppressor of Systemic RNA Silencing. *Viruses* 2017;9:E294.
62. Zhang C, Chen D, Yang G, Yu X, Wu J. Rice Stripe Mosaic Virus-Encoded P4 Is a Weak Suppressor of Viral RNA Silencing and Is Required for Disease Symptom Development. *Mol Plant Microbe Interact* 2020;33:412–422.
63. Qu F, Morris TJ. Suppressors of RNA silencing encoded by plant viruses and their role in viral infections. *FEBS Lett* 2005;579:5958–5964.
64. Carpino C, Ferriol Safont I, Elvira-González L, Medina V, Rubio L, *et al*. RNA2-encoded VP37 protein of Broad bean wilt virus 1 is a determinant of pathogenicity, host susceptibility, and a suppressor of post-transcriptional gene silencing. *Mol Plant Pathol* 2020;21:1421–1435.
65. Curaba J, Chen X. Biochemical activities of Arabidopsis RNA-dependent RNA polymerase 6. *J Biol Chem* 2008;283:3059–3066.
66. Peragine A, Yoshikawa M, Wu G, Albrecht HL, Poethig RS. SGS3 and SGS2/SDE1/RDR6 are required for juvenile development and the production of trans-acting siRNAs in Arabidopsis. *Genes Dev* 2004;18:2368–2379.

67. Mourrain P, Béclin C, Elmayan T, Feuerbach F, Godon C, *et al*. Arabidopsis SGS2 and SGS3 genes are required for posttranscriptional gene silencing and natural virus resistance. *Cell* 2000;101:533–542.

68. Béclin C, Boutet S, Waterhouse P, Vaucheret H. A branched pathway for transgene-induced RNA silencing in plants. *Curr Biol* 2002;12:684–688.